Journal of Physics D: Applied Physics

Direct Patterning of Nitrogen-Doped CVD Graphene Based Microstructures for Charge Carrier Measurements Employing Femtosecond Laser Ablation

To cite this article before publication: Nikolai G. Kovalchuk *et al* 2019 *J. Phys. D: Appl. Phys.* in press https://doi.org/10.1088/1361-6463/ab1c4b

Direct Patterning of Nitrogen-Doped CVD Graphene Based Microstructures for Charge Carrier Measurements Employing Femtosecond Laser Ablation

Nikolai G. Kovalchuk[1], Kiryl A. Niherysh[1], Andrei V. Felsharuk[1], Ivan A. Svito[2], Tomas Tamulevičius[3,4*], Sigitas Tamulevičius[3,4], Nikolai I. Kargin[5], Ivan V. Komissarov[1,5], Serghej L. Prischepa[1,5]

[1]Belarusian State University of Informatics and Radioelectronics, P. Browka Str. 6, 220013 Minsk, Belarus

[2]Belarusian State University, Nezalezhnastsi Av. 4, 220030, Minsk, Belarus

[3]Institute of Materials Science, Kaunas University of Technology, K. Baršausko Str. 59, LT-51423, Kaunas, Lithuania

[4]Department of Physics, Kaunas University of Technology, Studentų Str. 50, LT-51368, Kaunas, Lithuania

[5]National Research Nuclear University MEPhI, Kashirskoe Hwy. 31, Moscow, 115409, Russia

* mailto:tomas.tamulevicius@ktu.lt

Abstract

Chemical vapor deposited nitrogen-doped graphene, transferred on SiO_2/Si substrate was selectively patterned by femtosecond laser ablation for formation of the topology dedicated for charge carrier measurements. Ultrashort 1030 nm wavelength Yb:KGW fs-laser pulses of 22 μJ energy,14 mJ/cm^2 fluence, 96% pulse overlap and scanning speed of 100 mm/s were found to be optimum regime for the high throughput microstructure ablation in graphene, without surface damage of the substrate in the employed fs-laser micromachining workstation. Optical scanning

electron, atomic force microscopy as well as Raman spectroscopy were applied to clarify the intensive fs-laser light irradiation effects on graphene and substrate as well as to verify the quality of the graphene removal. Measurements of magnetotransport properties of the fs-laser ablated nitrogen-doped graphene microstructure in the Hall configuration enabled determination of the type as well as concentration of charge carriers in a wide temperature range.

Key words: Nitrogen doped graphene, femtosecond laser ablation, Hall resistance, charge carrier concentration

Introduction

The real two dimensional (2D) nature and unique electronic structure with linear dispersion make graphene very attractive material nowadays. However, the great application potential of graphene still faces the technological limitations, which results from the reduced dimensionality of graphene. Indeed, any impurities on graphene surface such as adsorbed oxygen, trapped water, chemical residuals cause change of its electronic state mainly due to the two mechanisms: charge transfer and charge scattering [1]. This may seriously affect the performance of designed electrical devices [2]. The top down approach widely used in modern electronics assumes application of conventional lithography, which is a multistep process and usually involves utilization of electron or light irradiation sensitive layers. As a result, the inevitable residuals of the resist on the surface of graphene change its electronic state [3]. Tremendous efforts usually are required to remove residuals of the resist completely [4, 5].

Direct patterning technique of graphene via ultrashort pulse laser ablation, which is considered as a prospective powerful tool in micro and nanofabrication of graphene-based devices [6], can be a competitive alternative to the conventional lithography process. It should be noted that the 2D nature of graphene, with charge carriers confined within one atomic layer, causes its electrical, optical and sensing properties to be strongly influenced by the surrounding media or functionalization of graphene. In this sense ultrashort pulse laser ablation appears as efficient technological solution in production of planar structures excluding any impurities or residuals

characteristic to different chemicals applied in conventional graphene patterning techniques. In contrast to the other serial exposure lithography techniques, like focused ion beam [7] and electron beam lithography [8, 9] microfabrication techniques based on ultrashort pulse laser approach [10, 11] widely accessible and easily scalable. Fs-laser micromachining demonstrates a diffraction limited patterning resolution, or even sub-wavelength resolution via direct laser interference patterning [12, 13], and at the same time promises a very competitive writing field area compared to conventional lithography techniques. One of the important parameters for the pulsed laser-assisted patterning is high peak power assured by the ultra-short pulse duration, which for the case of graphene ablation may vary from 10^{-15} [14-16] to 10^{-9} s [17]. Picosecond selective laser ablation of a wafer-scale graphene film was shown as flexible, high speed device fabrication method while avoiding the degradation of electrical properties associated with conventional lithographic method [18]. During last decade femtosecond (fs) lasers for micromachining technology have made their evolutionary step from scientific equipment to a reliable technological tool for industrial manufacturers. With their ability to process any material with a minimal amount of heat-affected zones and, as a result, with the increased resolution of the desired structures, fs-lasers are being considered for a growing list of micromachining applications.

Graphene-based micro and nanostructures could be considered as one of the evolving areas for variety of applications. As an example, micropatterning of CVD synthesized large area graphene films employing fs-laser cutting process could be mentioned [19]. It was shown that micro ribbon or other patterned micro structures can be fabricated without applying any resist. In [20] fs-laser ablation was reported as a part of technological process used to remove graphene from silicon-on-photonic integrated waveguides. Fs-laser ablation was shown as an efficient solution in some more sophisticated applications like graphene-based gas/vapor sensors that have attracted much attention in recent years due to their variety of structures, unique sensing performances [21].

Despite reasonably large number of papers [6, 19, 20, 22-24] addressed to the issue of single layer and/or multilayer graphene ablation, in many cases directly applying the regimes reported in the literature may not lead to the expected patterning results because it is both laser beam handling [25] and substrate material sensitive method.

The main issues to be solved for any practical applications, where graphene acts as a functional layer, are targeted removal of graphene with minimum damage of the substrate and

reasonable patterning speed. In the current research we have elucidated intensive light effects on the CVD grown bi-layer nitrogen-doped graphene transferred on SiO_2/Si substrate and optimized the fs-laser assisted patterning process. In particular, we found optimum relation between the fs-laser pulse energy, fluence and overlap of pulses. We successfully patterned the Hall structure with 80 μm width graphene strip employing fast galvanometric laser scanning setup. This gave us the opportunity, by conducting magnetotransport and electrical measurements at different temperatures and magnetic fields, to obtain information about the type and concentration of the charge carriers.

Experimental part

Graphene used in our work was grown by atmospheric pressure chemical vapor deposition (AP CVD) from chemically pure *n*-decane on a copper foil (Alfa Aesar) at 1050 °C utilizing a custom built setup. The samples were prepared in the presence of N_2 (99.95%) and H_2 (99.99%) gas flow with the rates of 100 and 6 cm^3/min, respectively. This approach allowed to synthesize the bi-layer graphene which was proved by the exhaustive analysis of Raman data [26]. After deposition, graphene was transferred on SiO_2(~700 nm)/Si substrate by wet transfer method. Detailed description of the graphene synthesis, transfer approach and graphene characterization can be found elsewhere [26, 27]. Comprehensive XPS analysis on identically synthesized samples revealed that graphene was N-doped with the nitrogen concentration of $n_N \approx 1.5\times10^{13}$ cm^{-2} [26].

Laser patterning was performed employing femtosecond Yb:KGW laser (λ = 1030 nm, τ = 270 fs, P = 4 W, Pharos 04-500-PP, Light Conversion) and micromachining workstation (FemtoLAB, Altechna R&D) controlled with the SCA software (Altechna R&D). Two modes of laser beam handling were utilized: (*i*) translation of the sample with respect to the tightly focused laser beam; (*ii*) steering of the beam with a galvo scanner with respect to the stationary sample. The former was exploited for elucidation of the intensive laser light interaction with the graphene on the SiO_2/Si substrates and determination of the laser processing conditions necessary to remove the graphene. Laser micromachining was performed with N.A. = 0.42 and 4 mm focal length 50× objective lens (Plan Apo NIR Infinity-Corrected, Mitutoyo) and XYZ translation stage (ANT130-160-XY, ANT130-5-V, Aerotech, further noted as XYZ).

The latter was applied for up scaling the patterning to cm^2 range areas and was based on a galvanometer scanner (SCANcube III 14, ScanLab) and F-theta lens of 100 mm focal length and 115 mm working distance (150-1001, Eksma Optics). A detailed description of both modes applied can be found elsewhere [28-31]. The diffraction limited spot sizes of the objective and F-theta lens focused laser beam were 2.54 μm and 14 μm, respectively. Using the first setup for evaluation of ablation parameters we made a test patterns of 10x10 μm in size. Two parameters were varied in our experiments, the fs-laser power (P = 0.69 mW - 20.7 mW) and the intershot distance (0.5 μm - 3.4 μm, or the pulse overlap from 80.3% to non-touching spots, respectively) resulting in an array of 30x30 spots. Power of the laser beam and distance between the neighboring exposed spots were gradually changed along vertical and horizontal lines, respectively (Figure 1 a). When applicable graphene removal conditions were obtained, the microstructure design for the Hall effect measurements was patterned employing the second, high throughput patterning laser setup using the recalculated parameters in order to keep the same level of the laser pulse energy (see Table 1). Differences in fluence per pulse due to different setups used (namely laser focusing conditions) were compensated increasing the pulse overlap.

Table 1 Laser processing conditions used in the experiments

Laser processing parameters	Laser beam steering method	
	XYZ	Galvo scanner
Pulse repetition rate (Hz)	200 000	
Average power (mW)	0.69 - 20.70, step 0.7	4.33
Energy per pulse (nJ)	3.5 - 103.5	21.7
Diffraction limited spot size (μm)	2.54	14.0
Fluence per pulse (mJ/cm^2)	68.1 – 2 041.0	14.1
Scanning speed (mm/s)	0.5	100
Intershot distance (μm)	0.5 - 3.4, step 0.1	2.5
Pulse density (pulses/mm)	294 – 2 000	400
Pulse overlap (%)	-33.9* - 80.3	96.4

*Negative values corresponds to non-overlapping separated points.

The patterned graphene structure was analyzed by optical microscopy (BXFM, Olympus), scanning electron microscopy (SEM, SU 9000, Hitachi), atomic force microscopy (AFM, Certus Light V, Nano Scan Technology) and Raman spectroscopy (Confotec NR 500, SOL Instruments, λ = 473 nm) to monitor structural changes under different fs-laser processing conditions. An 100× (numerical aperture NA = 0.95) objective and the laser power of 500 μW was used to collect the Raman signal. Mapping of the Raman signal was performed employing galvo scanner setup with spatial resolution smaller than 1 μm.

Magnetotransport measurements of fs-laser ablated bridge structure were performed in Hall geometry with 6 silver contacts as electric probes. Two contacts, along the bridge, were used for supplying the current and measuring the voltage (V_x) and while the other two perpendicular to the bridge were employed for Hall voltage measurements (V_H). DC resistivity and Hall measurements were carried out using a cryogen free measuring system (Cryogenic Ltd., London), which allows setting the sample temperature in the range from 2 to 300 K with an accuracy better than 0.05 K and magnetic field up to 8 T with central field homogeneity within 0.001% over 25 mm. The temperature was measured with a Cernox™ CX-1030 thermometer located on the holder near the sample. A Lakeshore 340 controller allowed stabilizing temperature with the accuracy of ±5 mK during the measurements.

DC resistivity was measured by the four-probe method with a Keithley 6430 Source-Measure Unit, which generated a DC current of 5 μA and measured the voltage. To measure the Hall voltage, a Keithley 2182A nanovoltmeter was used. Magnetic field was oriented perpendicular to the substrate surface and, hence, perpendicular to the current direction.

Results and discussion

Overview look of whole fs-laser ablated 30x30 matrix is depicted in Figure 1. From both, SEM (Figure 1 b) and optical microscope (Figure 1 c), micrographs one can directly observe a considerable correlation between the brightness or colors of the spots with respect to the laser power (along the vertical axis), and intershot distances (along the horizontal axis). In the area above the 9th row from the bottom (indicated with a "SiO_2" arrow in Figure 1 b) significant destruction of the sample surface is clearly noticeable. The 9th row in 30x30 matrix was obtained applying fluence of 613 mJ/cm^2. At the lower laser fluences used (68-545 mJ/cm^2, the corresponding rows from 1 to 8), some modification of the substrate is still visible, especially at higher pulse densities. Taking into account the pulse energy (21 nJ) and the diffraction limited laser spot size, the fluence per pulse level of 409 mJ/cm^2 was determined from SEM analysis as a good technological condition for selective graphene removal (indicated with a "G" arrow in Figure 1 c) using micromachining setup, where the sample was translated with respect to the laser beam. The graphene ablation threshold value identified here is close to the ones reported in literature [14, 24].

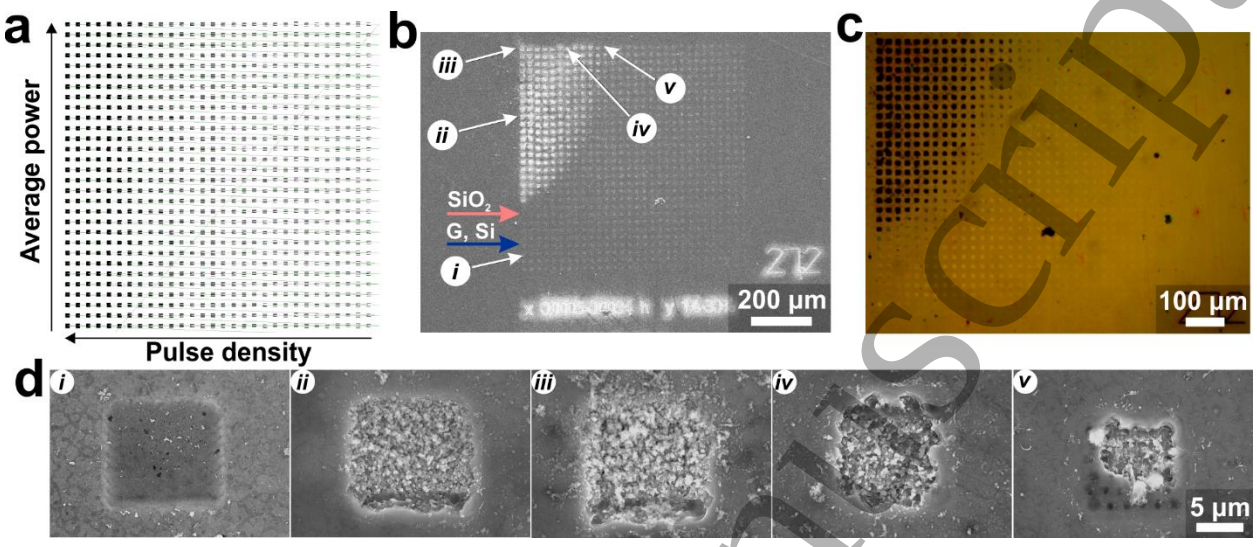

Figure 1 Fs-laser ablation of the test array pattern of 30x30 squares: (a) laser code screenshot from the SCA software, with arrows indicating the direction of the increasing pulse density and average laser power (fluence). (b) SEM micrograph, where horizontal arrows represent ablation fluence thresholds for SiO_2 (red, 4th row, 272 mJ/cm^2) and for graphene (blue, 9th row, 613 mJ/cm^2); numbers in circles indicate places depicted in (d) investigated under higher magnification. (c) Optical microscope micrograph. (d) Higher magnification SEM micrographs of single squares patterned under corresponding conditions: (i) 272 mJ/cm^2 fluence and 0.5 µm intershot distance (80.3% overlap); (ii) 1 430 mJ/cm^2, 0.5 µm (80.3%); (iii) 2 043 mJ/cm^2, 0.5 µm (80.3%), (iv) 2 043 mJ/cm^2, 2.8 µm (56.7%); (v) 2 043 mJ/cm^2, 3.4 µm (37.0%).

Zoomed-in SEM images of squares, patterned using different fs-laser processing conditions, are depicted in Figure 1 d. Indeed, above the ablation threshold of SiO_2 as well for high and low level of the beam overlap, a significant destruction of the substrate surface is observed (Figure 1 d ii, iii, iv, v). For the square patterned, at power level just below the one indicated with a red arrow in Figure 1 b, the substrate surface looks undamaged, whereas graphene layer is removed (Figure 1 d i). The estimated threshold fluence in the latter area of the array is smaller than the threshold of SiO_2 ablation, but taking into account transparency of SiO_2 and approximately two times smaller ablation threshold of Si, ~ 300 mJ/cm^2 [24], we may expect deterioration of top

SiO_2 layer via ablation of Si underneath. One could also notice that the SiO_2 thickness value in our case was from two to six time thicker compared to [24, 32], where fs-laser ablation thresholds were debated. From Figure 1 d one can see that the graphene layer seems intact only ~1.5-2 μm from the laser irradiated area indicating minimal heat affected zones achieved employing ultra-short pulse lasers. These findings are even more pronounced in the Raman analysis as discussed later on.

Since both Si and graphene have Raman active vibration modes, more quantitative information than just simple observation of fs-laser ablated Graphene/SiO_2/Si/ structure morphology can be obtained from Raman spectroscopy studies. One should keep in mind that the ratio of the intensity of the 2D peak to G peak, I_{2D}/I_G, indicates the presence of graphene as well as its quality [33] while the position of the silicon peak at 520.7 cm^{-1} can be employed to disclose the structural changes in silicon [34, 35]. In order to interpret the changes on the sample surface after the intensive laser light irradiation, systematic studies were performed employing Raman mapping of four characteristic laser ablated areas covering: (i) lowest, average and higher fluences at high pulse overlaps and (ii) area corresponding to minimal surface damage albeit visible changes according to microscopy study. This approach enabled us to reveal the laser effects on the sample at critical laser processing conditions and to relate the coverage of graphene together with Si destruction as a function of both fluence and pulse overlap. The summarized results are depicted in Figure 2.

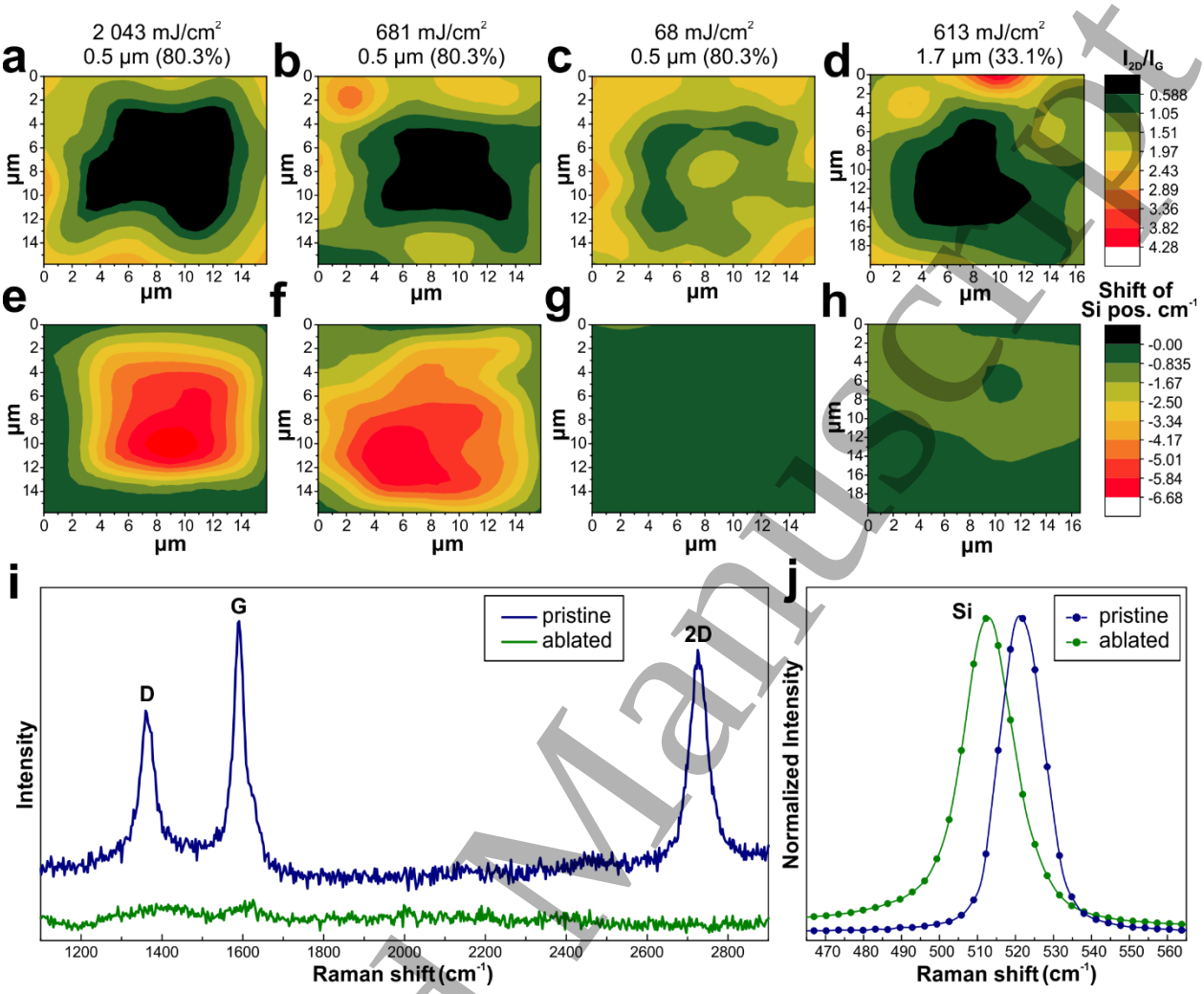

Figure 2 Micro Raman analysis. Contour plots of Raman analysis of the characteristic graphene line intensity ratio (I_{2D}/I_G, a-d) and red shift of the Si band position (e-h) of the laser ablated areas at different laser fluences and pulse overlaps indicated above the contour plots. Dark colored areas in (a), (b), (d) represent full removal of graphene, while red colored spots in (e), (f) correspond to damage of the substrate. Typical Raman spectra (i) and close up view at Silicon peak (j) of pristine and laser ablated samples analyzed in the contour plots (laser ablation conditions are the same like in (a), (e)).

As expected, for the highest value of fluence (>> 409 mJ/cm^2, determined from the microscopy analysis) I_{2D}/I_G contour plots (see Figure 2 a, b, d) indicate that no graphene is observed in the ablated area and at the same time the position of Si is strongly downshifted towards

lower wave numbers compared to crystalline Si (521 cm^{-1} see Figure 2 e, f) indicating damage of the substrate [34, 35]. The typical example of pristine and fs-laser ablated graphene spectra are depicted in Figure 2 i, j. In particular, the red shift of Raman Si band is shown in Figure 2 j and spectrum of the spectral region characteristic to graphene corresponding to completely ablated graphene is presented in Figure 2 i. For the intermediate energy density level (fluence 681 mJ/cm^2, overlap 80.3%), graphene is also removed, but the red shift of Si band position is still noticed, although it is less pronounced. Finally, for the lowest investigated energy density level (68 mJ/cm^2, 80.3%) no change in Si band position is visible (Figure 2 g). However, in this case graphene is removed only partially as indicated by the I_{2D}/I_G contour value of 0.59 (Figure 2 c). These discussed Raman results set us the range, where the energy density optimum condition for the graphene ablation is located i.e. fluence 409-681 mJ/cm^2 and pulse overlap 33.1%-80.3%, still preserving the quality of the substrate. These values are fully consistent with those obtained from the microscopy analysis (see Figure 1).

When the optimized graphene ablation conditions were obtained, a topology for Hall measurements was imposed for verification of fs-laser ablated graphene applicability for practical electrical measurements. For that purpose, we used graphene grown and transferred on SiO_2/Si substrate at the same conditions as for the experiment described above. The determined fs-laser ablation conditions were adapted for the galvo scanner-based beam steering setup preserving the necessary fluence level. The latter setup was chosen taking into account the macroscopic size of the graphene sample used in the electrical measurements (2x2 cm^2) and necessity of the fast fs-laser processing. An optical micrograph of the central part of the resulting microstructure is depicted in Figure 3 a. The continuity of the fs-laser patterned graphene strip was verified by Raman mapping technique as well. The I_{2D}/I_G contour plot of (Figure 3 b) revealed that, graphene in the bridge does not contain any holes or gaps, whereas no graphene remained outside the bridge. The AFM scans of the virgin SiO_2 surface, SiO_2 after graphene ablation under optimized conditions and graphene transferred on SiO_2, were acquired in tapping mode. The roughness analysis revealed that the morphology of SiO_2 after graphene ablation (average surface roughness R_a=0.55 nm) is determined by the overall morphology of the virgin surface - R_a=0.57 nm. Finally, the roughness of graphene was evaluated as R_a=0.56 nm. The AFM study is in line with the Raman mapping results and indicates that the surface of the substrate is preserved.

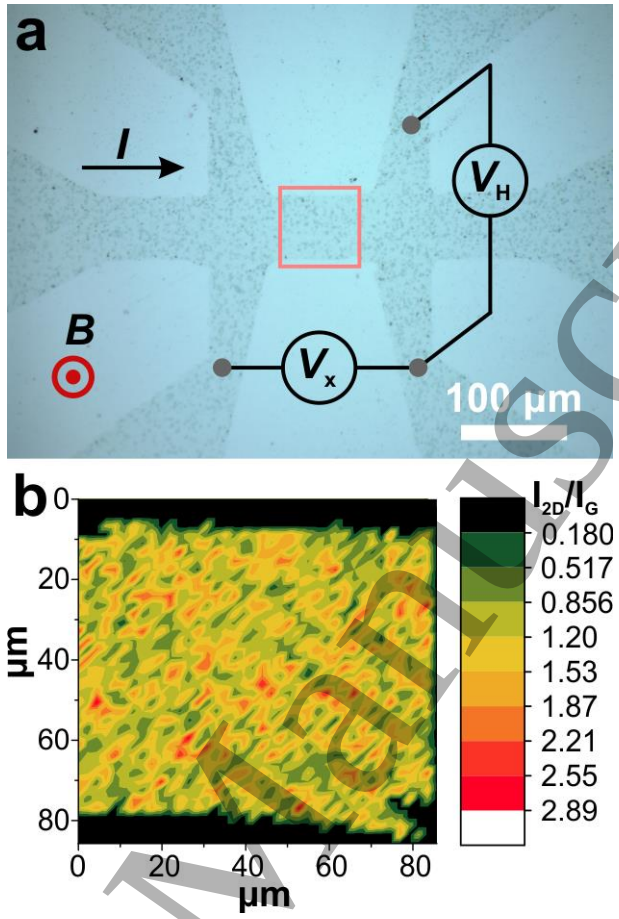

Figure 3 Graphene microstructure used for electrical Hall measurements. (a) the optical microscope image of the patterned graphene bridge and 6 contacts structure with the box indicating the area, where Raman mapping was performed, together with the wiring diagram and magnetic field (*B*) orientation used in the electrical measurements (*I* - direction of the current, V_x - voltage measurement along the bridge, V_H - voltage measurement across the bridge). (b) I_{2D}/I_G map of the graphene bridge structure (dark area corresponds to the contour where no graphene is present).

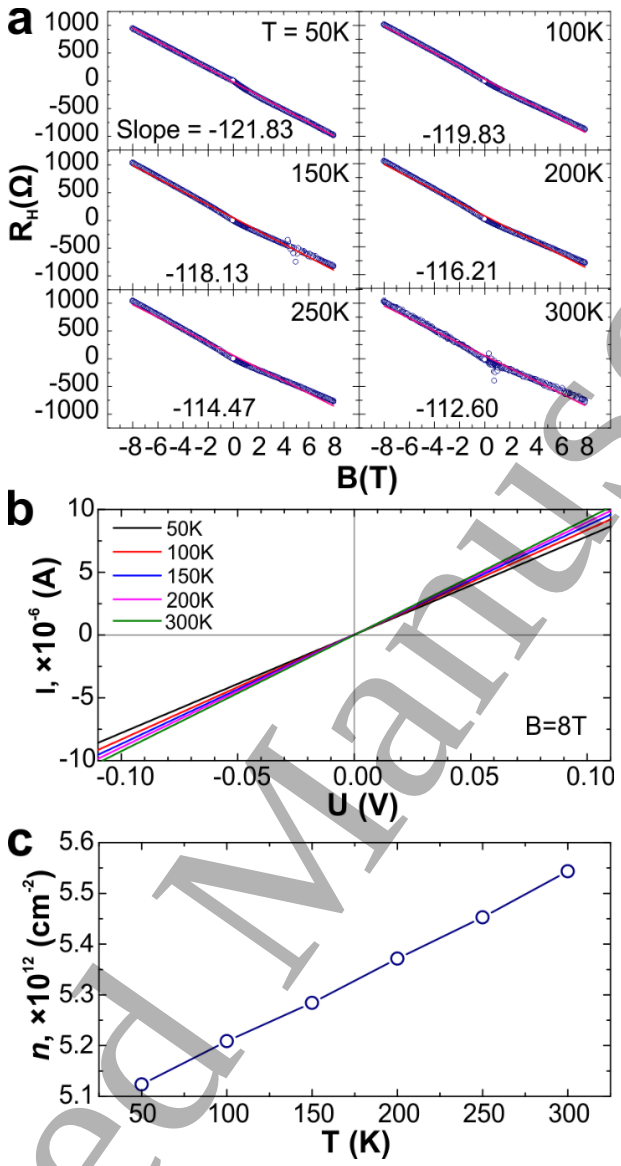

Figure 4 Electrical Hall measurements. (a) Measured Hall resistance R_H versus magnetic field at different temperatures (symbols) together with the linear fits (lines). The slopes of linear fits are indicated for each temperature. (b) Current-voltage characteristics measured at different temperatures ranging from 50 K to 300 K at constant magnetic inductance B=8 T. (c) Charge carrier concentration extracted from resistive Hall measurements at different temperatures.

In addition to the demonstration of the ability for the direct fs-laser patterning technique of graphene, the present paper also illustrates the applicability of such structure for the evaluation of the charge carrier concentration. In this work we measured Hall resistance R_H as a function of B at

different T. These results are depicted in Figure 4a. The experimental $R_H(B)$ dependencies are well fitted by linear approximation. Applying the standard relation for the carrier concentration n from the Hall effect measurements, $n=q^{-1}(B/R_H)$, q being the elementary charge, one can evaluate the n values at different temperatures. This result is shown in Figure 4c. It follows that the carrier concentration slightly varies between 5.1×10^{12} cm^{-2} at T= 50 K and 5.55×10^{12} cm^{-2} at T= 300 K, which is in good agreement with what it should be expected for N-doped graphene [36]. Taking into account mutual directions of the external magnetic field and biasing current used in our configuration, we may conclude that the main type of carriers in our nitrogen-doped graphene are holes (p-type).

The main advantage of the structure produced in our case is that graphene was not contaminated by polymer [5] as usually occurs in patterning utilizing conventional lithography. Current-voltage characteristics measured at different temperatures T and constant magnetic inductance B revealed a linear relationships (Figure. 4 b), which confirms the absence of leakage currents through the oxide layer into the substrate.

It is generally accepted that the type of charge carriers in N-doped graphene depends on the configuration that the embedded nitrogen atoms form. It is known that graphitic and pyrolic configuration lead to n-type, whereas pyridinic and nitrilic configuration leads to p-type [37]. In our earlier work [26] we have demonstrated that according to XPS analysis of graphene synthesized at identical conditions, it contained N atom concentration of $n_N \approx 1.5 \times 10^{13}$ cm^{-2}. Comparing this value with the charge carrier concentration value obtained from the Hall measurements we may conclude that the average number of holes transferred by nitrogen, n/n_N, is 0.37 per atom at room temperature. This value is very close to what is known for pyridinic N-bond type, 0.45 [37]. For nitrilic bonding this value is higher, 0.66 [37]. From this we one could suppose that the probable chemical N-bonding is pyridinic. However, we need to emphasize that evaluation of exact n/n_N value for graphene requires the elimination of charged transfer effect caused by substrate, trapped water during the graphene transfer, etc. which is hardly achievable and is out of the scope of this work.

Conclusions

It was demonstrated that bilayer graphene can be effectively removed by fs-laser ablation (fluence per pulse14.1 mJ/cm^2) at relatively high laser beam positioning speed of 100 mm/s in cm^2 areas employing galvoscanner beam steering without damaging the SiO_2/Si substrate.

Micro Raman analysis elucidated typical effects, correspondent to femtosecond laser irradiation energy densities of the Graphene/SiO_2/Si samples, that were also visible as morphology changes under microscopy analysis.

The fs-laser patterned graphene microstructures demonstrated themselves as applicable for the electrical Hall resistivity measurements that were used in order to obtain the carrier type and their concentration: *p*-type and 5.5x10^{12} cm^{-2}, respectively.

Acknowledgments

Authors are grateful for BSc student Linas Šimatonis and MSc student Orestas Ulčinas for their help with laser ablation experiments and Dr. Sergey M. Zavadski for AFM measurements. I.V.K and S.L.P. acknowledge financial support of the "Improving of the Competitiveness" Program of the National Research Nuclear University MEPhI. T.T. and S.T. acknowledges funding of a Joint Lithuanian–Latvian–Chinese (Taiwanese) Tripartite Cooperation Programme project co-financed by the Research Council of Lithuania (Grant No. S-LLT-18-2) and the Ministry of Science and Technology of Taiwan (Contract SV3-0618).

References

[1] S. Das Sarma, S. Adam, E.H. Hwang, E. Rossi, Electronic transport in two-dimensional graphene, Reviews of Modern Physics 83(2) (2011) 407-470.
[2] A. Pirkle, J. Chan, A. Venugopal, D. Hinojos, C.W. Magnuson, S. McDonnell, L. Colombo, E.M. Vogel, R.S. Ruoff, R.M. Wallace, The effect of chemical residues on the physical and electrical properties of chemical vapor deposited graphene transferred to SiO2, Applied Physics Letters 99(12) (2011) 3.
[3] J.W. Suk, W.H. Lee, J. Lee, H. Chou, R.D. Piner, Y.F. Hao, D. Akinwande, R.S. Ruoff, Enhancement of the Electrical Properties of Graphene Grown by Chemical Vapor Deposition via Controlling the Effects of Polymer Residue, Nano Letters 13(4) (2013) 1462-1467.
[4] Y. Chen, X.L. Gong, J.G. Gai, Progress and Challenges in Transfer of Large-Area Graphene Films, Advanced Science 3(8) (2016) 15.

[5] N.G. Kovalchuk, K.A. Nigerish, M.M. Mikhalik, N.I. Kargin, I.V. Komissarov, S.L. Prischepa, Possibility of Determining the Graphene Doping Level Using Raman Spectra, Journal of Applied Spectroscopy 84(6) (2018) 995-998.
[6] R. Sahin, E. Simsek, S. Akturk, Nanoscale patterning of graphene through femtosecond laser ablation, Applied Physics Letters 104(5) (2014) 4.
[7] D.C. Bell, M.C. Lemme, L.A. Stern, J. Rwilliams, C.M. Marcus, Precision cutting and patterning of graphene with helium ions, Nanotechnology 20(45) (2009) 5.
[8] L. Tapaszto, G. Dobrik, P. Lambin, L.P. Biro, Tailoring the atomic structure of graphene nanoribbons by scanning tunnelling microscope lithography, Nature Nanotechnology 3(7) (2008) 397-401.
[9] Y.W. Tan, Y. Zhang, H.L. Stormer, P. Kim, Temperature dependent electron transport in graphene, European Physical Journal-Special Topics 148 (2007) 15-18.
[10] R.S. Gonnelli, F. Paolucci, E. Piatti, K. Sharda, A. Sola, M. Tortello, J.R. Nair, C. Gerbaldi, M. Bruna, S. Borini, Temperature Dependence of Electric Transport in Few-layer Graphene under Large Charge Doping Induced by Electrochemical Gating, Scientific Reports 5 (2015) 8.
[11] B. Davaji, H.D. Cho, M. Malakoutian, J.K. Lee, G. Panin, T.W. Kang, C.H. Lee, A patterned single layer graphene resistance temperature sensor, Scientific Reports 7 (2017) 10.
[12] T. Roch, E. Beyer, A. Lasagni, Surface modification of thin tetrahedral amorphous carbon films by means of UV direct laser interference patterning, Diamond and Related Materials 19(12) (2010) 1472-1477.
[13] L. Guo, H.B. Jiang, R.Q. Shao, Y.L. Zhang, S.Y. Xie, J.N. Wang, X.B. Li, F. Jiang, Q.D. Chen, T. Zhang, H.B. Sun, Two-beam-laser interference mediated reduction, patterning and nanostructuring of graphene oxide for the production of a flexible humidity sensing device, Carbon 50(4) (2012) 1667-1673.
[14] W. Zhang, L. Li, Z.B. Wang, A.A. Pena, D.J. Whitehead, M.L. Zhong, Z. Lin, H.W. Zhu, Ti:sapphire femtosecond laser direct micro-cutting and profiling of graphene, Applied Physics a-Materials Science & Processing 109(2) (2012) 291-297.
[15] J.H. Yoo, J.B. In, J.B. Park, H.J. Jeon, C.P. Grigoropoulos, Graphene folds by femtosecond laser ablation, Applied Physics Letters 100(23) (2012) 3.
[16] C. Cheng, R.Y. He, C. Romero, J.R.V. de Aldana, F. Chen, Spontaneous micro-modification of single-layer graphene induced by femtosecond laser irradiation, Applied Physics Letters 111(24) (2017) 5.
[17] A.M. Perez-Mas, P. Alvarez, N. Campos, D. Gomez, R. Menendez, Graphene patterning by nanosecond laser ablation: the effect of the substrate interaction with graphene, Journal of Physics D-Applied Physics 49(30) (2016) 7.
[18] D.M.A. Mackenzie, J.D. Buron, P.R. Whelan, B.S. Jessen, A. Silajdzic, A. Pesquera, A. Centeno, A. Zurutuza, P. Boggild, D.H. Petersen, Fabrication of CVD graphene-based devices via laser ablation for wafer-scale characterization, 2d Materials 2(4) (2015) 6.
[19] G. Kalita, L.T. Qi, Y. Namba, K. Wakita, M. Umeno, Femtosecond laser induced micropatterning of graphene film, Materials Letters 65(11) (2011) 1569-1572.
[20] J. Van Erps, T. Ciuk, I. Pasternak, A. Krajewska, W. Strupinski, S. Van Put, G. Van Steenberge, K. Baert, H. Terryn, H. Thienpont, N. Vermeulen, Laser ablation- and plasma etching-based patterning of graphene on silicon-on-insulator waveguides, Optics Express 23(20) (2015) 26639-26650.

[21] T. Wang, D. Huang, Z. Yang, S.S. Xu, G.L. He, X.L. Li, N.T. Hu, G.L. Yin, D.N. He, L.Y. Zhang, A Review on Graphene-Based Gas/Vapor Sensors with Unique Properties and Potential Applications, Nano-Micro Letters 8(2) (2016) 95-119.
[22] I. Bobrinetskiy, A. Emelianov, A. Nasibulin, I. Komarov, N. Otero, P.M. Romero, Photophysical and photochemical effects in ultrafast laser patterning of CVD graphene, Journal of Physics D-Applied Physics 49(41) (2016) 7.
[23] A. Roberts, D. Cormode, C. Reynolds, T. Newhouse-Illige, B.J. Leroy, A.S. Sandhu, Response of graphene to femtosecond high-intensity laser irradiation, Applied Physics Letters 99(5) (2011) 3.
[24] T.Q. Dong, M. Sparkes, C. Durkan, W. O'Neill, Evaluating femtosecond laser ablation of graphene on SiO2/Si substrate, Journal of Laser Applications 28(2) (2016) 6.
[25] A. Gil-Villalba, R. Meyer, R. Giust, L. Rapp, C. Billet, F. Courvoisier, Single shot femtosecond laser nano-ablation of CVD monolayer graphene, Scientific Reports 8 (2018) 6.
[26] I.V. Komissarov, N.G. Kovalchuk, V.A. Labunov, K.V. Girel, O.V. Korolik, M.S. Tivanov, A. Lazauskas, M. Andrulevicius, T. Tamulevicius, V. Grigaliunas, S. Meskinis, S. Tamulevicius, S.L. Prischepa, Nitrogen-doped twisted graphene grown on copper by atmospheric pressure CVD from a decane precursor, Beilstein Journal of Nanotechnology 8 (2017) 145-158.
[27] I.V. Komissarov, N.G. Kovalchuk, E.A. Kolesov, M.S. Tivanov, O.V. Korolik, A.V. Mazanik, Y.P. Shaman, A.S. Basaev, V.A. Labunov, S.L. Prischepa, N.I. Kargin, R.V. Ryzhuk, S.A. Shostachenko, Micro Raman Investigation of Graphene Synthesized by Atmospheric Pressure CVD on Copper Foil from Decane, Physics Procedia 72 (2015) 450-454.
[28] E. Adomavičiūtė, T. Tamulevičius, L. Šimatonis, E. Fataraitė-Urbonienė, E. Stankevičius, S. Tamulevičius, Micro-structuring of Electrospun Mats Employing Femtosecond Laser, Materials Science-Medziagotyra 21(1) (2015) 44-51.
[29] I. Antanaviciute, L. Simatonis, O. Ulcinas, A. Gadeikyte, B. Abakeviciene, S. Tamulevicius, V. Mikalayeva, V.A. Skeberdis, E. Stankevicius, T. Tamulevicius, Femtosecond laser micro-machined polyimide films for cell scaffold applications, Journal of Tissue Engineering and Regenerative Medicine 12(2) (2018) E760-E773.
[30] T. Tamulevicius, L. Simatonis, O. Ulcinas, S. Tamulevicius, E. Zukauskas, R. Rekuviene, L. Mazeika, Micromachining and validation of the scanning acoustic microscope spatial resolution and sensitivity calibration block for 20-230 MHz frequency range, Microscopy 65(5) (2016) 429-437.
[31] M. Juodenas, T. Tamulevicius, O. Ulcinas, S. Tamulevicius, Implementation of an optimized microfluidic mixer in alumina employing femtosecond laser ablation, Journal of Micromechanics and Microengineering 28(1) (2018) 10.
[32] T. Rublack, M. Muchow, S. Hartnauer, G. Seifert, Laser ablation of silicon dioxide on silicon using femtosecond near infrared laser pulses, Proceedings of the Siliconpv 2011 Conference (1st International Conference on Crystalline Silicon Photovoltaics) 8 (2011) 467-472.
[33] A.C. Ferrari, D.M. Basko, Raman spectroscopy as a versatile tool for studying the properties of graphene, Nature Nanotechnology 8(4) (2013) 235-246.
[34] M. Benyoucef, M. Kuball, J.M. Sun, G.Z. Zhong, X.W. Fan, Raman scattering and photoluminescence studies on Si/SiO2 superlattices, Journal of Applied Physics 89(12) (2001) 7903-7907.

[35] W.-G. Ding, J. Yuan, L.-H. Meng, S.-J. Wu, W. Yu, G.-S. Fu, Dependence of Optical Absorption in Silicon Nanostructures on Size of Silicon Nanoparticles, Communications in Theoretical Physics 55(4) (2011) 688-692.
[36] M. Scardamaglia, C. Struzzi, S. Osella, N. Reckinger, J.F. Colomer, L. Petaccia, R. Snyders, D. Beljonne, C. Bittencourt, Tuning nitrogen species to control the charge carrier concentration in highly doped graphene, 2D Materials 3(1) (2016) 8.
[37] T. Schiros, D. Nordlund, L. Palova, D. Prezzi, L.Y. Zhao, K.S. Kim, U. Wurstbauer, C. Gutierrez, D. Delongchamp, C. Jaye, D. Fischer, H. Ogasawara, L.G.M. Pettersson, D.R. Reichman, P. Kim, M.S. Hybertsen, A.N. Pasupathy, Connecting Dopant Bond Type with Electronic Structure in N-Doped Graphene, Nano Letters 12(8) (2012) 4025-4031.